THE COMPUTATION OF FIELDS AND SIGNALS DUE TO FERROMAGNETIC ANOMALIES

Harold A. Sabbagh and L. David Sabbagh

Sabbagh Associates, Inc.
2634 Round Hill Lane
Bloomington, IN 47401

INTRODUCTION

In this paper we develop a model for the computation of electromagnetic fields in anomalous regions of ferromagnetic cylinders. The role of electric and magnetic current densities as sources for these fields is explicitly presented. The starting point for the development is the computation of a three-dimensional Green's function for the cylinder, from which the appropriate integral relations between the field and its sources can be derived. The rigorous calculation of the anomalous current source within the anomalous region requires the solution of an integral equation that has the Green's function as its kernel. We do not carry out this calculation, but approximate the anomalous current by the applied field due to the exciting coil (which, for our examples is an infinite solenoid that is coaxial to the cylinder). Once the field within the anomalies is determined, the field external to the wall of the tube may be computed, and this provides the signal that is sensed by a coil, or other means.

The anomalies may be either holes or cracks, which affect both the local electrical conductivity and magnetic permeability, or magnetic 'hard spots', which may alter the magnetic permeability, but not the electrical conductivity. We will give examples of the computed fields and signals for a simple slot-like anomaly. These results are useful in the quantitative nondestructive evaluation of ferromagnetic cylinders and other structures.

MAXWELL'S EQUATIONS

Let the permeability of the host material material be μ_0 (not necessarily free space), and the conductivity be σ_0. The corresponding parameters within the anomalous region are μ_f and σ_f. Then Maxwell's equations for the perturbed field are:

$$\begin{aligned} \nabla \times (\mathbf{E}_0 - \mathbf{E}_f) &= -j\omega\mu_0(\mathbf{H}_0 - \mathbf{H}_f) - j\omega(\mu_0 - \mu_f)\mathbf{H}_f \\ \nabla \times (\mathbf{H}_0 - \mathbf{H}_f) &= \sigma_0(\mathbf{E}_0 - \mathbf{E}_f) + j\omega\epsilon_0(\mathbf{E}_0 - \mathbf{E}_f) + (\sigma_0 - \sigma_f)\mathbf{E}_f. \end{aligned} \tag{1}$$

The last term in each of the right-hand sides acts as a source for the perturbed field, the top source being the anomalous magnetic current density, and the bottom the familiar anomalous electric current density. The solution for the perturbed field is

$$(\mathbf{H}_0 - \mathbf{H}_f)(\mathbf{r}) = \iiint \mathbf{G}^{(e)}(\mathbf{r}|\mathbf{r}') \cdot \mathbf{E}_f(\mathbf{r}')(\sigma_0 - \sigma_f)(\mathbf{r}') - \mathbf{G}^{(m)}(\mathbf{r}|\mathbf{r}') \cdot j\omega\mathbf{H}_f(\mathbf{r}')(\mu_0 - \mu_f)(\mathbf{r}')d\mathbf{r}', \tag{2}$$

where $\mathbf{G}^{(e,m)}(\mathbf{r}|\mathbf{r}')$ is the dyadic Green's function for the host region, and the volume of

integration is over the anomalous region, for which $\sigma_0 - \sigma_f \neq 0$, $\mu_0 - \mu_f \neq 0$. The superscripts (e,m) denote an electric source and magnetic source, respectively. Equation (2) provides a rigorous way of computing the unknown fields, $\mathbf{E}_f$, $\mathbf{H}_f$, within the anomaly, but to simplify the calculations we simply replace these fields under the triple integral by $\mathbf{E}_0$, $\mathbf{H}_0$, which are the known fields due to the exciting source. For relatively small flaws, we have found this to be a reasonable approximation.

COMPUTATION OF THE GREEN'S FUNCTION

Clearly, the most important part of the integral solution, (2), is the Green's function, so we will outline a method for computing it in cylindrical coordinates. First, we write each field variable as a 2D Fourier transform in (ϕ, z)

$$G(r,\phi,z) = \sum_{n=-\infty}^{\infty} e^{jn\phi} \int_{-\infty}^{\infty} \tilde{G}(r,n,h) e^{jhz} dh, \tag{3}$$

and then transform Maxwell's equations into an equivalent matrix form for the transverse field components in Fourier transform space:

$$\frac{d}{dr}\begin{pmatrix} \tilde{E}_z \\ r\tilde{E}_\phi \\ \tilde{H}_z \\ r\tilde{H}_\phi \end{pmatrix} = \begin{pmatrix} 0 & 0 & a_{11}(r) & a_{12}(r) \\ 0 & 0 & a_{21}(r) & a_{22}(r) \\ b_{11}(r) & b_{12}(r) & 0 & 0 \\ b_{21}(r) & b_{22}(r) & 0 & 0 \end{pmatrix} \begin{pmatrix} \tilde{E}_z \\ r\tilde{E}_\phi \\ \tilde{H}_z \\ r\tilde{H}_\phi \end{pmatrix} + \begin{pmatrix} u_{11} & 0 & 0 & 0 & u_{15} & 0 \\ u_{21} & 0 & 0 & 0 & 0 & u_{26} \\ 0 & u_{32} & 0 & u_{34} & 0 & 0 \\ 0 & 0 & u_{43} & u_{44} & 0 & 0 \end{pmatrix} \begin{pmatrix} \tilde{J}_r \\ \tilde{J}_\phi \\ \tilde{J}_z \\ \tilde{M}_r \\ \tilde{M}_\phi \\ \tilde{M}_z \end{pmatrix}, \tag{4}$$

where

$$a_{11} = \frac{jhn}{\omega\hat{\epsilon}r},\ a_{12} = \left(\frac{-jh^2}{\omega\hat{\epsilon}r} + \frac{j\omega\mu}{r}\right),\ a_{21} = \left(\frac{jn^2}{\omega\hat{\epsilon}r} - j\omega\mu r\right),\ a_{22} = \frac{-jnh}{\omega\hat{\epsilon}r},$$

$$b_{11} = \frac{-jhn}{\omega\mu r},\ b_{12} = \left(\frac{jh^2}{\omega\mu r} - \frac{j\omega\hat{\epsilon}}{r}\right),\ b_{21} = \left(-\frac{jn^2}{\omega\mu r} + j\omega\hat{\epsilon}r\right),\ b_{22} = \frac{jnh}{\omega\mu r}, \tag{5}$$

$$u_{11} = -\frac{h}{\omega\hat{\epsilon}},\ u_{15} = 1,\ u_{21} = -\frac{n}{\omega\hat{\epsilon}},\ u_{26} = -r,$$

$$u_{32} = -1,\ u_{34} = -\frac{h}{\omega\mu},\ u_{43} = r,\ u_{44} = -\frac{n}{\omega\mu}.$$

The $\tilde{J}$'s are the impressed electric current sources, and the $\tilde{M}$'s are the impressed magnetic current sources. The derivation of the matrix form is straightforward, thoug algebraically tedious.

When the sources are set equal to zero, the resulting homogeneous vector-matrix equation has certain eigenvector solutions:

$$\begin{pmatrix} \tilde{E}_z \\ r\tilde{E}_\phi \\ \tilde{H}_z \\ r\tilde{H}_\phi \end{pmatrix} = \bar{v}_1,\ \bar{v}_2,\ \bar{v}_3,\ \bar{v}_4, \tag{6}$$

where

$$\bar{v}_1=\begin{pmatrix} J_n(\alpha r) \\ -\frac{hn}{\alpha^2}J_n(\alpha r) \\ 0 \\ -\frac{j\omega\hat{\varepsilon}}{\alpha}rJ_n'(\alpha r)\end{pmatrix},\bar{v}_2=\begin{pmatrix} H_n^{(2)}(\alpha r) \\ -\frac{hn}{\alpha^2}H_n^{(2)}(\alpha r) \\ 0 \\ -\frac{j\omega\hat{\varepsilon}}{\alpha}rH_n^{(2)\prime}(\alpha r)\end{pmatrix},\bar{v}_3=\begin{pmatrix} 0 \\ \frac{j\omega\mu}{\alpha}rJ_n'(\alpha r) \\ J_n(\alpha r) \\ -\frac{hn}{\alpha^2}J_n(\alpha r)\end{pmatrix},\bar{v}_4=\begin{pmatrix} 0 \\ \frac{j\omega\mu}{\alpha}rH_n^{(2)\prime}(\alpha r) \\ H_n^{(2)}(\alpha r) \\ -\frac{hn}{\alpha^2}H_n(2)(\alpha r)\end{pmatrix}. \tag{7}$$

Note that $\bar{v}_1$ and $\bar{v}_2$ are Transverse Magnetic (TM) modes, and $\bar{v}_3$ and $\bar{v}_4$ are Transverse Electric (TE) modes. J_n and H_n are, respectively, the usual Bessel and Hankel functions.

The Green's function is expanded in terms of these eigenvectors, as shown in Figure 1. In this figure we divide the cylinder into three regions: the interior (I), the wall (II) and the exterior (III). The notation, $G(r,\phi,z;r',\phi',z')_{ij}$, for the Green's function means that the field point, (r,ϕ,z), is in region i (I, II, or III), and the source point, (r',ϕ',z'), is in region j (I, II, or III). Hence, Figure 1(a) shows the computation of G_{12} and Figure 1(b) shows the computation of G_{21}.

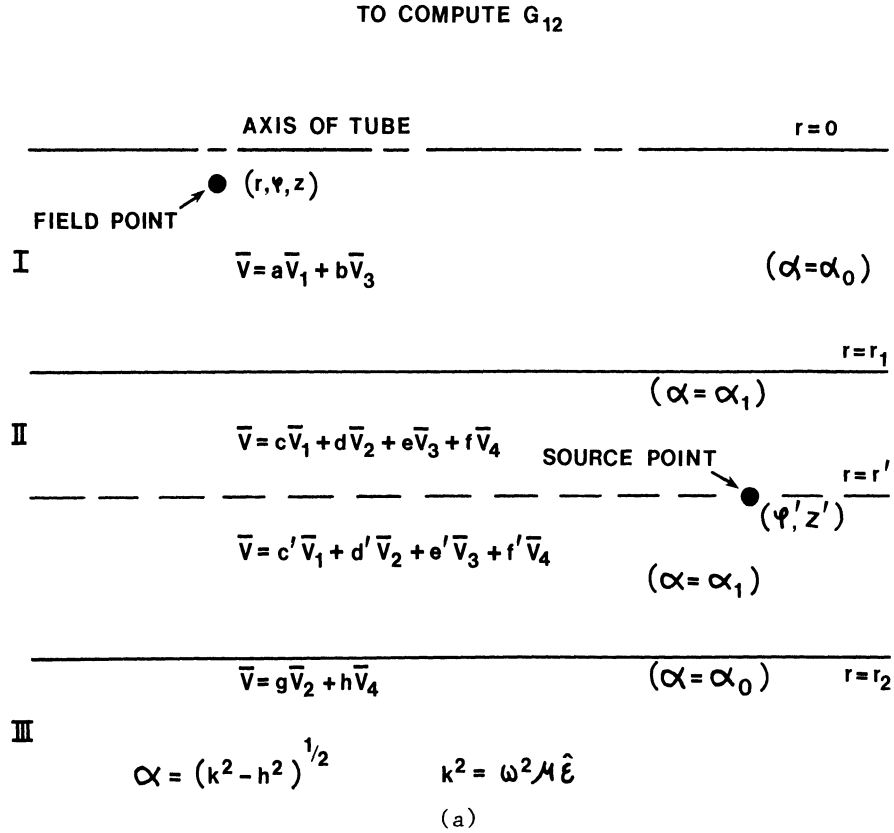

Fig. 1 Computation of Green's function: (a) G_{12}.

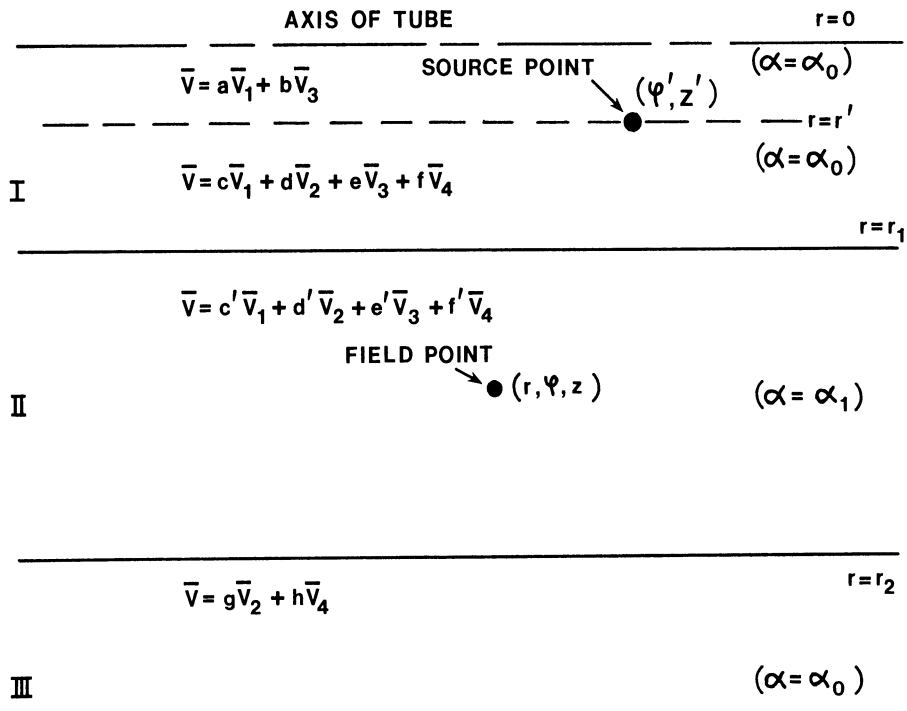

(b)

Fig. 1 Computation of Green's Function (b) G_{21}.

The transformed Green's function suffers a jump discontinuity across the cylinder, $r = r'$, which can be calculated by using the following argument: the source for the Green's function is a delta function, $\delta(\phi - \phi')\delta(z - z')\delta(r - r')/r'$, of electric or magnetic current at (r', ϕ', z'). The two dimensional Fourier transform (in (ϕ, z)) of the product of the first two delta functions is $(1/(2\pi)^2)e^{-jn\phi'}e^{-jhz'}$, so that the right-hand side of (4) is

$$\overline{\overline{U}}\,\hat{\bar{J}}\,\frac{e^{-jm\phi'}e^{-jhz'}}{(2\pi)^2}\,\frac{\delta(r - r')}{r'}, \tag{8}$$

where $\overline{\overline{U}}$ is the matrix that multiplies the source vector in (4), and $\hat{\bar{J}}$ is a unit vector of either electric or magnetic current. Integrate the matrix equation (4) an epsilon distance across $r = r'$:

$$\bar{v}^{(+)} - \bar{v}^{(-)} = \frac{\overline{\overline{U}}}{r'}\,\hat{\bar{J}}\,\frac{e^{-jm\phi'}e^{-jhz'}}{(2\pi)^2}. \tag{9}$$

This is the ''jump discontinuity'' in computing the Green's function in the Fourier domain.

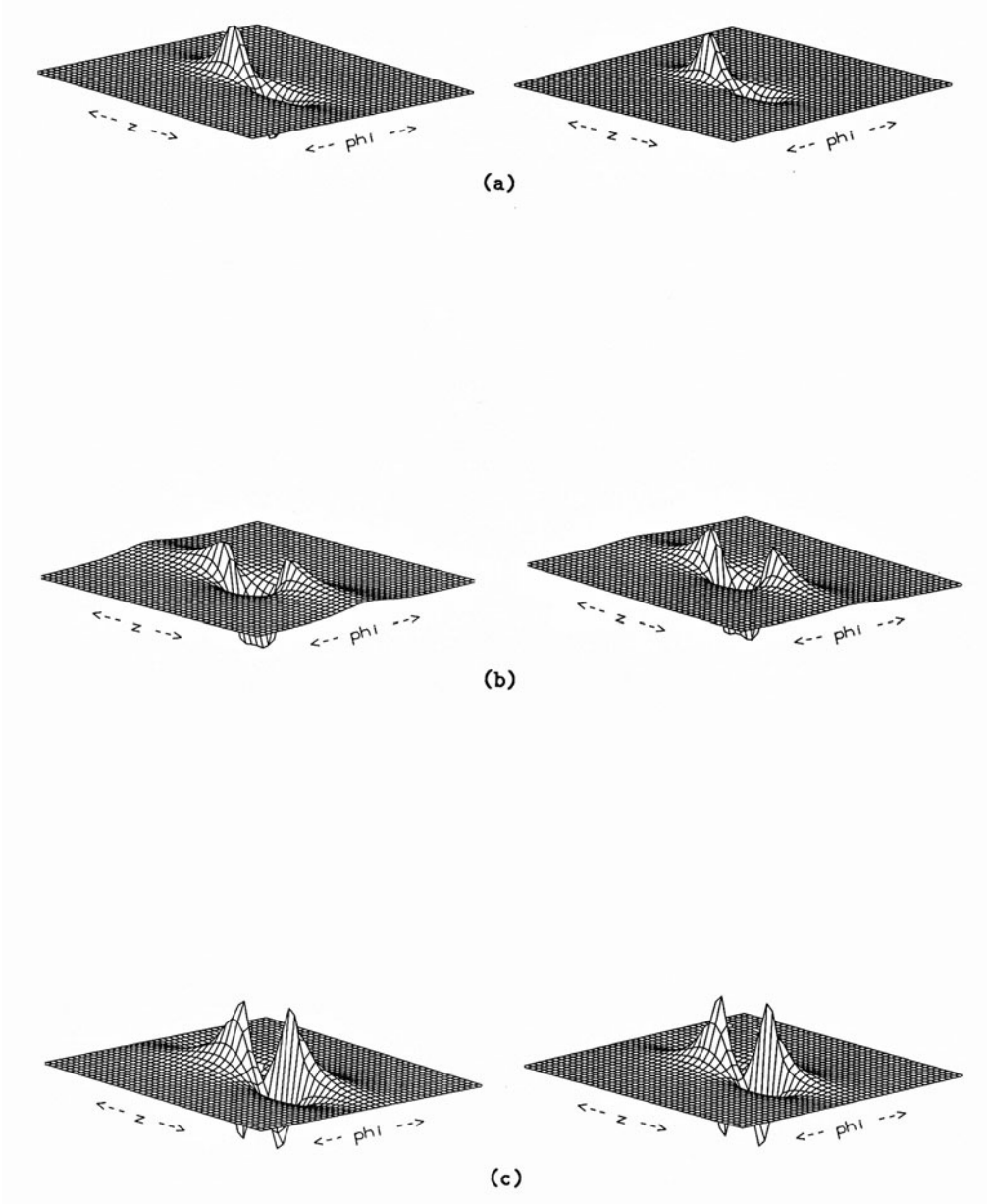

Fig. 2 Complex **H** field. The left-hand figure is the real part and the right-hand the imaginary. (a) Radial component, (b) axial component, (c) azimuthal component.

With this background it is very straightforward to compute the expansion coefficients $(a - h,\ c' - f')$ shown in Figure 1. The algebra becomes a little tedious, and it is convenient to do the computations numerically on the computer. Indeed, the advantage of working in the Fourier transform domain is that the analytic calculations amount to little more than algebra, and are easily done.

EXAMPLES OF FIELD CALCULATIONS

Once the Fourier-transformed Green's function is obtained, we substitute it into the Fourier-transformed version of (2) (with the exciting fields substituted for the true fields under the integral sign) and continue to work in the transform domain. The final results in physical space are obtained by taking an inverse transform, using a fast Fourier transform algorithm. In the work described here, we have used Singleton's mixed radix algorithm [1]. This algorithm is easily adapted to multidimensional problems and does not require that the number of transform points be a power of two. We have used 256 points in the z direction and 360 in the ϕ direction.

The model flaw (or anomaly) is a notch whose length along the z axis is 0.200 inch, depth into the wall 0.0385 inch (starting at the interior surface of the cylinder) and width in the ϕ direction is 0.022 inch. The host material is assumed to have a permeability, $\mu = 70 \times \mu_0$, and a conductivity of $\sigma = 1.4 \times 10^6$. The outer diameter of the cylinder is 7/8 inch and the wall thickness is 0.048 inch. The excitation source is an infinite solenoid that is coaxial with the cylinder, and the excitation frequency is 100 kHz.

We have calculated the complex magnetic field vector, $\mathbf{H}$, that exists 30 mils from the inner wall; in Figure 2 are illustrated the real and imaginary parts of the field components due to an equivalent anomalous electric current source within the flaw. The results for an equivalent anomalous magnetic current source are virtually identical and are not shown.

The radial field component (Figure 2(a)) is odd in z (because the flaw is symmetrical) and even in ϕ. This component peaks at the edges of the flaw, whereas the axial component (which is even in both dimensions, as shown in Figure 2(b)) has a broad major peak at the center of the flaw, and smaller, sharper peaks at each edge. Finally, the ϕ component, which is shown in Figure 2(c), is odd in both variables and peaks at the four corners of the rectangular notch. These results are helpful in developing inversion algorithms for eddy-current reconstructions.

ACKNOWLEDGEMENT

This work was supported by the U. S. Department of Energy under Contract No. DE-AC02-83ER80096 with Sabbagh Associates, Inc.

REFERENCES

[1] Digital Signal Processing Committee, IEEE Acoustics, Speech, and Signal Processing Society, *Programs for Digital Signal Processing*, New York: IEEE Press, 1979, pp. 1.4-1 to 1.4-18.